Journal of Materials Chemistry C

ROYAL SOCIETY OF CHEMISTRY

PAPER

Water-soluble ZnSe/ZnS:Mn/ZnS quantum dots convert UV to visible light for improved Si solar cell efficiency†

Cite this: DOI: 10.1039/d0tc04580b

Hisaaki Nishimura,[a] Takaya Maekawa,[a] Kazushi Enomoto,[b] Naoteru Shigekawa,[a] Tomomi Takagi,[c] Susumu Sobue,[c] Shoichi Kawai[c] and Dae Gwi Kim *[a]

Received 24th September 2020,
Accepted 1st December 2020

DOI: 10.1039/d0tc04580b

rsc.li/materials-c

The sensitivity of Si solar cells to the UV portion of the solar spectrum is low, and must be increased to further improve their efficiencies. In this study, water-soluble ZnSe/ZnS:Mn/ZnS core/shell/shell quantum dots (QDs) capable of converting UV into visible light were synthesised by a hydrothermal method. A photoluminescence quantum yield of 84% was achieved by carefully investigating and optimising the QD preparation conditions. Furthemore, we prepared wavelength-conversion glass containing the ZnSe/ZnS:Mn/ZnS QDs dispersed in sol–gel glass and applied it to Si solar cells. As a result, the spectral sensitivity of the Si solar cell at wavelengths shorter than 400 nm was significantly improved, and the amount of power generated (conversion efficiency) was increased by 7.4% compared with that of the cell without the wavelength-conversion glass coating.

Introduction

Silicon solar cells, as the current most popular solar cell type, account for approximately 90% of the total solar cell market share.[1] Some crystalline Si solar cells with conversion efficiencies close to 25% have been developed.[2–4] Although Si solar cells have a high spectral sensitivity towards visible through near-infrared wavelengths of the solar spectrum, their spectral sensitivity to UV light, approximately 10% of sunlight, is low. The energy conversion efficiency of Si solar cells can be further improved by addressing this issue, for which using phosphor-based wavelength-conversion films has become an effective approach.[5–7] Thus far, down-shifting UV to visible light and up-shifting infrared to visible light have been extensively investigated for wavelength conversion.[7–22] However, it is difficult to achieve strong up-conversion luminescence due to the low optical excitation density of sunlight.[21,22] Therefore, down-shifting wavelength-conversion materials are favourable, for which organic dyes,[8–10] rare-earth complexes,[11–16] and semiconductor quantum dots (QDs)[17–20] have been studied as potential phosphors. Klampaftis *et al.* improved the conversion efficiency of polycrystalline Si solar cells from 15.07% to 15.35% using an EVA polymer containing an organic dye with an emission peak at 413 nm as a wavelength-conversion material.[8] Iso *et al.* fabricated wavelength-conversion films containing rare-earth complexes (YVO4:Bi^{3+},Eu^{3+}) with a photoluminescence quantum yield (PLQY) of 21.4% and combined them with Si solar cells.[11] As a result, under UV and near-infrared irradiation, the energy conversion efficiency of the solar cell was increased by 3.19% as compared to that of the sample without phosphor. However, under AM1.5G simulated solar irradiation, the energy conversion efficiency was reduced because the reflectance in the visible region was increased by the wavelength-conversion film. Beak *et al.* succeeded in increasing the conversion efficiency of p-type Si solar cells from 16.92% to 18.00% using a wavelength-conversion film spin-coated on Si nitride with $Cd_{0.5}Zn_{0.5}S$/ZnS QDs to achieve a PLQY of 80%.[17] Wang *et al.* reported that Mn-doped $CsPbCl_3$ QDs, with a large Stokes shift of over 1 eV and a quantum yield of 62%, were coated on multi-crystalline Si solar cells, leading to an increased conversion efficiency of 6.2%.[18] They also reported that control of the surface structures was an important factor in improving the solar cell characteristics.[23] Wavelength-conversion materials for solar cells must possess not only a high PLQY but also suitable anti-photobleaching properties.[24] Generally, although organic dyes and rare-earth complexes have high PLQYs, their anti-photobleaching properties are lower than those of semiconductor QDs based on inorganic materials.[25,26] Meanwhile, semiconductor QDs are inferior to organic dyes in terms of PLQY; however, such QDs could have significant potential as wavelength-conversion materials if their

[a] Department of Applied Physics, Osaka City University, Osaka 558-8585, Japan. E-mail: tegi@a-phys.eng.osaka-cu.ac.jp
[b] RIKEN Center for Emergent Matter Science (CEMS), Saitama 351-0198, Japan
[c] Advanced Research and Innovation Center, Denso Corporation, 500-1 Minamiyama, Komenoki-cho, Nisshin, Aichi 470-0111, Japan

† Electronic supplementary information (ESI) available. See DOI: 10.1039/d0tc04580b

PLQYs were to be improved because of their favourable anti-photobleaching properties.[25] CdSe QDs, which have a narrow size distribution and extremely high PLQY, have been actively studied as a model material to synthesise semiconductor QDs and investigate their optical properties.[27] However, since the band-edge photoluminescence (PL) comprises most of the PL band, the PL and absorption spectra overlap. Therefore, re-absorption becomes a problem in applying CdSe QDs as wavelength-conversion materials. Furthermore, CdSe QDs absorb visible light, which reduces the incident light intensity to the solar cell and decreases the energy conversion efficiency. Therefore, wavelength-conversion materials for Si solar cells must be made of an inorganic material with suitable anti-photobleaching properties, have an absorption edge wavelength shorter than 400 nm, have limited absorption–PL spectral overlap, and have a high PLQY. $CuInS_2$ and $AgInS_2$ QDs have low absorption-PL overlap, *i.e.*, a large Stokes shift.[28] However, their absorption onset is in the near-infrared to visible region, where the spectral sensitivity of Si solar cells is high. Therefore, it is desirable to use materials that absorb only wavelengths shorter than 400 nm to significantly reduce the spectral sensitivity of Si-type solar cells. Fabricating semiconductor QDs that absorb only UV light requires semiconductor materials with large bandgap energies. For example, since ZnSe has a bandgap energy of 2.7 eV, the absorption onset wavelength can be adjusted to 400 nm by preparing ZnSe QDs. However, ZnSe QDs generally exhibit band-edge PL with a small Stokes shift in the blue region, where the spectral sensitivity of Si solar cells is low. To address this, it is effective to dope QDs with impurities such as Mn^{2+} or Cu^{2+} as emission centres to emit visible light, where the spectral sensitivity of Si solar cells is high.

For example, in semiconductor QDs doped with Mn^{2+} as emission centres, the QD excitation energy transfers to Mn^{2+}, resulting in orange emission (Mn-related PL (Mn PL)) due to the intra 3*d*-shell $^4T_1 \rightarrow {}^6A_1$ transition of Mn^{2+}. In other words, Mn^{2+}-doped ZnSe (ZnSe:Mn^{2+}) QDs can convert UV to orange light ($\sim$600 nm, $\sim$2.1 eV). Therefore, ZnSe:Mn^{2+} QDs hold significant potential as wavelength-conversion materials for Si solar cells.[29,30] Thus far, semiconductor QDs doped with impurities have been extensively investigated for application as new functional materials.[31–33] Gan *et al.* reported the synthesis of ZnSe:Mn QDs with a PLQY of 50% by a nucleation-doping method.[34] In recent times, Yang *et al.* developed a synthesis scheme for $Zn_{1-x}Mn_xSe$ QDs (x = 0.001–0.5) involving a reaction in a 1-octadecene solution at high temperatures.[35]

To apply colloidal QDs to wavelength-conversion materials for Si solar cells, they must be dispersed in matrices such as polymer films or glasses.[36] Glasses are stable and transparent bulk materials, making them suitable for use as wavelength-conversion films.[36,37] The sol–gel method is a well-known approach for dispersing colloidal QDs in glasses.[36–39] Li *et al.* reported a method for uniformly dispersing CdTe QDs in silica-based sol–gel glasses prepared by the hydrolysis of 3-aminopropyltrimethoxysilane.[36] To uniformly disperse QDs in a glass, the sol–gel silica and colloidal QDs must be mixed well. Since QDs synthesised by the hot-injection method are hydrophobic, it is difficult for them to disperse in sol–gel glasses. Thus, water-soluble QDs are desirable. One method to prepare water-soluble QDs involves the ligand-exchange reaction of oil-soluble QDs synthesised by the hot-injection method.[40,41] Selvaraj *et al.* prepared water-soluble ZnSe:Mn/ZnS core/shell nanorods with a PLQY of 49% *via* the ligand exchange process.[42] However, this process was known to degrade the PL properties of oil-soluble QDs.[40] Therefore, the direct synthesis of water-soluble QDs remained important. Aboulaich *et al.* reported on the synthesis of water-soluble ZnSe:Mn and ZnSe:Mn/ZnS core/shell QDs with PLQYs of 3.5% and 9%, respectively, using a reflux method.[43] Hardzei *et al.* successfully synthesised ZnSe:Mn/ZnS core/shell QDs with PLQYs of 10% using a hydrothermal method.[44] However, the PLQYs of these samples are much lower than those of QDs synthesised by the hot-injection method. Therefore, it was necessary to synthesise water-soluble Mn-doped ZnSe QDs with higher PLQYs. In previous studies on the synthesis of water-soluble Mn-doped ZnSe QDs, most samples emitted weak Mn PL. In particular, we prepared ZnSe:Mn QDs in a previous work, wherein the core ZnSe QD was directly doped with Mn^{2+}, but their PLQY was only approximately 20%.[29] In contrast, hydrothermally synthesised non-doped ZnSe QDs and ZnSe/ZnS QDs exhibit high PLQYs of over 60% and 90%, respectively.[45] The major difference between the PLQYs of ZnSe and ZnSe:Mn QDs is considered the pH of the precursor solution, which is well known as an essential parameter in the hydrothermal synthesis of semiconductor QDs.[46,47] The optimum pH for the synthesis of the ZnSe QDs has been reported as 6.[45] In contrast, if ZnSe:Mn QDs are synthesised at pH 6, no Mn PL is observed, *i.e.*, Mn^{2+} cannot be doped.[29] The use of an alkaline precursor solution enables Mn^{2+} doping, wherein a ZnSe:Mn precursor at pH 10 yields the highest Mn PL.[29] However, the PLQY of ZnSe QDs synthesised under alkaline conditions is low.[46] In other words, the condition necessary for Mn^{2+} doping (pH 10) is significantly different from the optimum condition for preparing the host ZnSe QDs to suppress non-radiative recombination processes (pH 6). This is the reason for the low PLQYs of ZnSe:Mn QDs. Additionally, it is also difficult to dope QDs with impurities like Mn^{2+} due to self-purification, wherein impurities are removed during QD growth.[32,48,49] Thus, new strategies are needed to synthesise Mn-doped ZnSe QDs with strong Mn PL.[50–52] Wood *et al.* reported the synthesis of oil-soluble ZnSe/ZnS:Mn/ZnS QDs with a PLQY of 65% by forming ZnS:Mn inner-shell and ZnS outer-shell layers on the surface of ZnSe-core QDs using a hot-injection method.[50] Luong *et al.* also reported the preparation of water-soluble ZnSe/ZnS:Mn/ZnS core/shell/shell QDs by a reflux method, but their PLQY remained low at 42.9%.[52]

In this study, we focused on the Mn^{2+} doping of the shell layer instead of directly doping the core QDs of the ZnSe host (Fig. 1a). To apply water-soluble ZnSe/ZnS:Mn/ZnS core/shell/shell QDs as wavelength-conversion materials and improve the conversion efficiency of Si solar cells, the PLQY must be maximised. Therefore, we investigated the preparation conditions of the ZnSe/ZnS:Mn/ZnS QDs using *N*-acetyl-L-cysteine

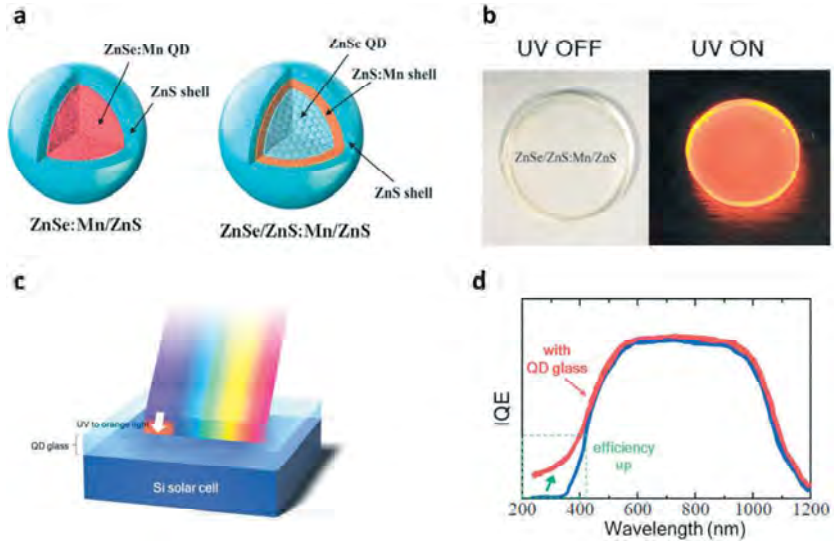

Fig. 1 Concept of the present study. (a)Schematic of ZnSe:Mn/ZnS core/shell QDs and ZnSe/ZnS:Mn/ZnS core/shell/shell QDs. (b) Photographs of the QD wavelength-conversion glass under room light and UV irradiation. The glass is transparent under room light and emits orange light under UV. (c) Schematic configuration of a solar cell combined with the QD wavelength-conversion glass. Visible light passes through the QD glass, while UV light is converted into orange light that reaches the solar cell. (d) Demonstration of how UV light can be used to improve the power generation.

(NAC)-capped ZnSe QDs, which have the highest PLQY among aqueous ZnSe QDs reported thus far, as the core QDs, and finally succeeded in increasing the PLQY to 84%. The prepared QDs were then dispersed in a sol–gel glass to fabricate highly luminescent wavelength-conversion glass with a transmissivity over 90% in the visible region (Fig. 1b). The conversion efficiency of the Si solar cells with the wavelength-conversion glass was improved by 7.4% (Fig. 1c and d), which is the highest conversion efficiency improvement yet achieved for Si solar cells using wavelength-conversion materials.

Experimental section

Preparation of ZnSe precursor solution

The ZnSe precursor solution was prepared by the method reported by Lee *et al.*[45] Briefly, $Zn(ClO_4)_2{\cdot}6H_2O$ (1.0 mmol) and *N*-acetyl-L-cysteine (NAC) (2.4 mmol) as a ligand were dissolved in 50 mL of deionised (DI) water. The pH of the solution was adjusted to 8.5, and a freshly prepared solution of NaHSe (0.2 mmol) was added. Then, the pH was adjusted to 6.0 by adding diluted HCl.

Preparation of ZnS:Mn precursor solution

The ZnS:Mn precursor solution was prepared by adding a Mn^{2+} source to the ZnS precursor solution. $Zn(ClO_4)_2{\cdot}6H_2O$ (1.2 mmol) and NAC (8.4 mmol) were dissolved in 20 mL of DI water. Subsequently, NaOH was added to adjust the pH to 4.0, and $Na_2S{\cdot}9H_2O$ (0.24 mmol) and $Mn(ClO_4)_2{\cdot}6H_2O$ (0.15 mmol) were added. To determine the optimum conditions, we prepared ZnS:Mn precursor solutions with different molar ratios of Zn^{2+}, NAC, and Mn^{2+}.

Preparation of ZnS precursor solution

The ZnS precursor solution was prepared as follows. First, NAC (7.2 mmol) was dissolved in 50 mL of DI water, then $Zn(ClO_4)_2{\cdot}6H_2O$ (3.0 mmol) was added as a Zn^{2+} source. Subsequently, NaOH was added to this solution to adjust the pH to 4.0, and $Na_2S{\cdot}9H_2O$ (0.6 mmol) was added. The pH of the ZnS precursor solution was then adjusted to different values to determine the optimal conditions.

Synthesis of ZnSe/ZnS:Mn/ZnS core/shell/shell QDs

Firstly, ZnSe core QDs were prepared by the hydrothermal method reported by Lee *et al.*[45,46] The ZnSe precursor solution (10 mL) was loaded into an autoclave and incubated at 200 °C for 60 min. The PLQY of the ZnSe-core QDs was 60%.[46] To synthesise the ZnSe/ZnS:Mn/ZnS core/shell/shell QDs, ZnS:Mn and ZnS shells were prepared by microwave-assisted hydrothermal synthesis.[46] The ZnS:Mn precursor solution was then added to the prepared ZnSe core QD solution, and ZnSe/ZnS:Mn core/shell QDs were synthesised by microwave irradiation for 2 min at 120 °C using a single-mode CEM Discover system. To determine the optimal amount of ZnS:Mn precursor, the ZnSe core QD solution and ZnS:Mn precursor solution were mixed at different ratios. Finally, the ZnS precursor was added to the ZnSe/ZnS:Mn core/shell QD solution, and ZnSe/ZnS:Mn/ZnS core/shell/shell QDs were synthesised under microwave irradiation at 140 °C. The ZnS precursor was added gradually in five steps and heated to fix the total amount of added ZnS:Mn and ZnS precursors. The heating time was gradually increased to 4, 4, 6, 6, and 10 min.

Preparation of wavelength-conversion glass

The wavelength-conversion glass was prepared by dispersing the ZnSe/ZnS:Mn/ZnS QDs in sol–gel glass according to a

previously reported method.[37] A mixed solution of 11 mM aqueous citric acid (2 mL) and 3-aminopropyltrimethoxysilane (2 mL) was stirred in a Teflon chalet (φ = 34 mm) for 24 h to promote hydrolysis. To concentrate the QD solution, the ZnSe/ZnS:Mn/ZnS QDs were precipitated by adding 2-propanol to the QD solution, and the solution was centrifuged at 3500 rpm for 20 min. The precipitates were then re-dispersed with DI water to increase the concentration by 10 times. Subsequently, 1 mL of an aqueous solution containing the ZnSe/ZnS:Mn/ZnS QDs and 0.3 mL of an additional Zn^{2+} solution (0.48 mmol of $Zn(ClO_4)_2{\cdot}6H_2O$ and 2.40 mmol of NAC mixed in 10 mL of DI water) were added to the sol–gel solution. The obtained samples were applied to the Si solar cells and dried in the dark. The thickness of the wavelength-conversion glass was 200 μm.

Chemicals

For the experiment, $Zn(ClO_4)_2{\cdot}6H_2O$ and $Mn(ClO_4)_2{\cdot}6H_2O$ were purchased from Fujifilm Wako Chemicals, and selenium (99.999%) was purchased from Aldrich. Furthermore, $Na_2S{\cdot}9H_2O$ was purchased from Kisida Chemical, and 3-aminopropyltrimethoxysilane was purchased from Tokyo Kasei.

Characterisation and spectroscopic measurements

The absorption spectra were obtained using a JASCO V-650 UV-Vis spectrophotometer with a spectral resolution of 0.5 nm. The PL spectra were measured with a JASCO FP-8300 spectrofluorometer at an excitation wavelength of 325 nm and a spectral resolution of 0.5 nm, and the PL intensity of each sample was determined by dividing the PL intensity by the absorption intensity at the excitation wavelength. The absolute PLQY was measured using a JASCO ILF-835 100 mm integrating sphere system coupled with the spectrofluorometer. To measure the PL decay profiles, the third-harmonic-generated light (355 nm) from a laser-diode-pumped yttrium aluminium garnet laser with a pulse duration of 20 ns and a repetition rate of 20 Hz was used as the excitation source. The PL decay profiles were observed using a 500 MHz digitising oscilloscope. High-resolution electron microscopy images were obtained using a JEOL JEM-2100F/SP. Energy-dispersive X-ray spectroscopy (EDX) was also performed to estimate the actual doping amount of Mn^{2+}. The field emission scanning electron microscopy (FE-SEM) image was obtained using a JEOL JSM-6500F.

Evaluation of solar cell characteristics

The Si solar cell modules (10 mm × 10 mm, η = 20.0 ± 1.1%) were fabricated by K-I-S (Japan). The solar cell module with wavelength-conversion glass was fabricated by dropping the sol–gel solution onto the cell, then drying in a flat, dark location. The droplet volume of the sol–gel solution was adjusted such that the film thickness after drying was 200 μm. The *I–V* curves (Wacom electric, WXS-156S-10, AM1.5 G 100 mW cm^{-2}) and EQE (Bunkoukeiki, SM-250CE, 1.0 mW cm^{-2}) were estimated using a solar simulator. The surface reflectance of the Si solar cell modules was determined using a QE-R3011 (Enli Technology Co., Ltd).

Results and discussion

Fig. S1 (ESI†) shows the absorption and PL spectra of the ZnSe:Mn/ZnS core/shell QDs prepared from a pH 10 ZnSe:Mn precursor solution. The PL spectrum consists of a PL band originating from the intra-3d shell transition of Mn^{2+} with a peak near 2.1 eV and band-edge PL. The PLQY of the ZnSe:Mn QDs was 20%, which was increased to 30% by introducing a ZnS shell onto the surfaces. Although the PLQY was improved by preparing ZnSe:Mn/ZnS core/shell QDs, further increasing the PLQY requires a fundamental improvement in the synthetic method. Here, instead of directly doping Mn^{2+} into the ZnSe-core QDs, as described above, non-doped ZnSe QDs prepared under optimal conditions were used as host QDs. Then, the ZnS:Mn shell was introduced using an alkaline precursor solution. Finally, to improve the PLQY, a ZnS capping layer was applied to yield multi-shell ZnSe/ZnS:Mn/ZnS core/shell/shell QDs.

Fig. 2 shows the absorption and PL spectra of the ZnSe/ZnS:Mn/ZnS core/shell/shell QDs synthesised as follows. First, the ZnS:Mn precursor solution was prepared with a Zn^{2+} : S^{2-} : NAC : Mn^{2+} molar ratio of 1.0 : 0.2 : 4.8 : 0.1 at pH 10.5. Then, the ZnSe-core QD solution and ZnS:Mn precursor solution were mixed at a [ZnS : Mn]/[ZnSe] ratio of 1.0 based on the molar ratio of Zn^{2+} in each solution. The mixed solution was heated by microwave irradiation to prepare ZnSe/ZnS:Mn core/shell QDs. Subsequently, ZnSe/ZnS:Mn/ZnS core/shell/shell QDs were prepared by adding a ZnS outer shell precursor solution and heating by microwave irradiation. As shown in Fig. 2, these QDs have a stronger Mn PL than the ZnSe:Mn/ZnS QDs. In other words, this method is effective for synthesising Mn-doped ZnSe QDs. In the ZnSe/ZnS:Mn/ZnS core/shell/shell QDs, however, band-edge PL was also clearly observed because of the presence of many non-doped ZnSe/ZnS QDs. Therefore, we attempted to optimise each synthesis step according to the following four conditions: the amount of added ZnS:Mn precursor, the pH of the ZnS outer shell precursor, the [NAC]/[Zn] molar ratio in the ZnS : Mn precursor, and the concentration of Mn^{2+} in the ZnS:Mn precursor. Fig. S2 (ESI†) shows the flowchart of the optimisation experiments. The integrated Mn

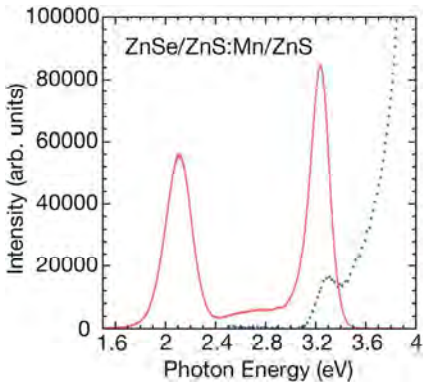

Fig. 2 Absorption (blue dashed line) and PL (red solid line) spectra of the ZnSe/ZnS:Mn/ZnS core/shell/shell QDs.

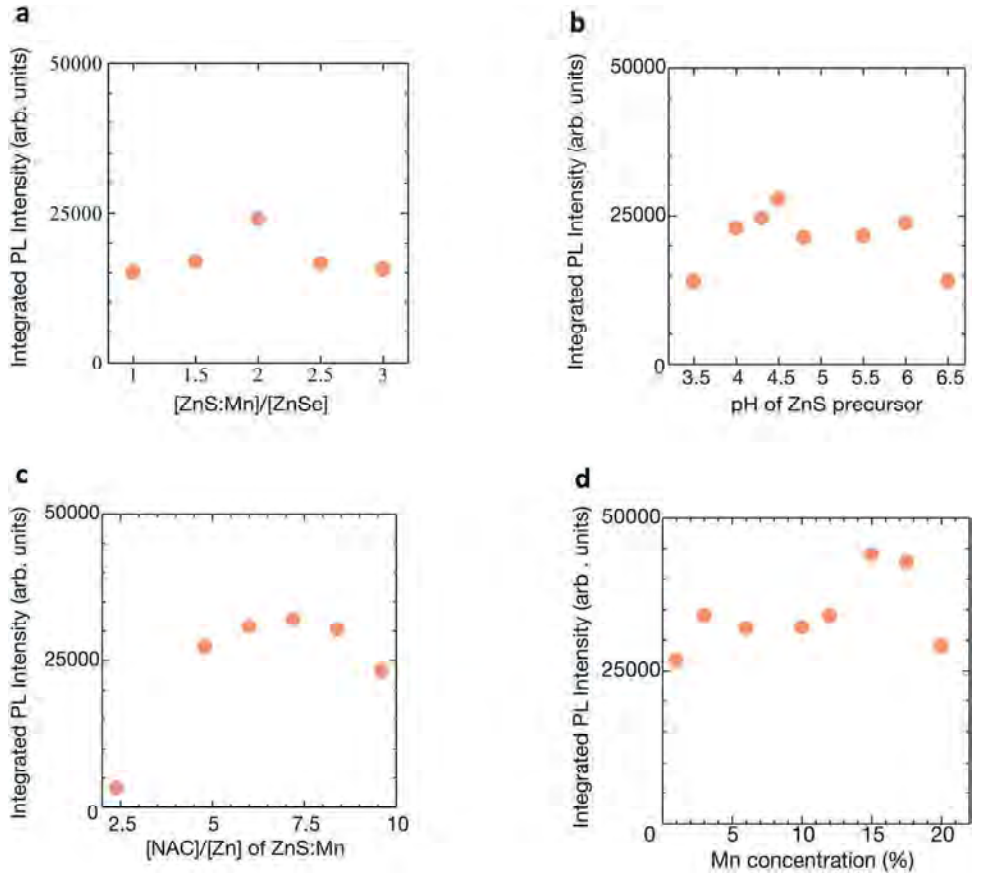

Fig. 3 Integrated Mn PL intensity of ZnSe/ZnS:Mn/ZnS core/shell/shell QDs. Dependence of Mn PL intensity on the (a) [ZnS:Mn]/[ZnSe] ratio, (b) pH of the ZnS precursor, (c) [NAC]/[Zn] molar ratio of the ZnS:Mn precursor, and (d) Mn concentration of the ZnS:Mn precursor.

PL intensities for each condition are plotted in Fig. 3a–d, and the PL spectra are shown in Fig. S3 (ESI†). The excitation wavelength was fixed at 325 nm. The PL intensity of each sample was compared by dividing the PL intensity by the absorption intensity at the excitation wavelength. Therefore, the relative PLQY of each sample can be compared.

First, we investigated the dependence of the Mn PL intensity on the mixing ratio of the ZnSe-core QD solution and ZnS:Mn precursor solution, which was defined by the molar ratio of Zn ions contained in each one ([ZnS:Mn]/[ZnSe]). Here, the Mn concentration, defined as the molar ratio of Zn and Mn ions in the ZnS:Mn precursor solution, was fixed at 10%. The pH of the ZnS outer shell precursor was fixed at 6.0. Fig. 3a shows the integrated Mn PL intensity for [ZnS : Mn]/[ZnSe] = 1.0, 1.5, 2.0, 2.5, and 3.0, showing that the maximum was obtained for [ZnS:Mn]/[ZnSe] = 2.0.

Next, the dependence of the Mn PL intensity on the pH of the ZnS outer shell precursor was investigated. ZnSe/ZnS:Mn/ZnS core/shell/shell QDs were synthesised using ZnS precursors at pH 3.5, 4.0, 4.3, 4.5, 4.8, 5.5, 6.0, and 6.5. The [ZnS:Mn]/[ZnSe] ratio was fixed to 2.0. As shown in Fig. 3b, the optimal ZnS precursor pH was found to be 4.5.

To determine the optimum [NAC]/[Zn] molar ratio in the ZnS:Mn precursor solution, we synthesised ZnSe/ZnS:Mn/ZnS core/shell/shell QDs at [NAC]/[Zn] = 2.4–9.6. As shown in Figure S3c, band-edge PL was recognised to be dominant under the condition of [NAC]/[Zn] = 2.4. It is well known that ligands play a major role in QD synthesis. Therefore, in this study, we also investigated the [NAC]/[Zn] molar ratio in detail. It was considered that the band-edge PL became strong because the escape of Mn from the QDs due to the self-purification effect could not be suppressed when [NAC]/[Zn] = 2.4. When [NAC]/[Zn] > 4.8, the band-edge-PL intensity decreased, and Mn PL became dominant. Fig. 3c shows the Mn PL intensity as a function of [NAC]/[Zn], illustrating that the maximum was observed at [NAC]/[Zn] = 7.2.

Finally, we investigated the dependence of the Mn PL intensity on the Mn concentration of the ZnS:Mn shell precursor. Fig. 3d shows the Mn-PL intensity of the ZnSe/ZnS:Mn/ZnS core/shell/shell QDs prepared at Mn concentrations between 1% and 20%, illustrating that the maximum was observed at 15%.

From the above, the optimum conditions for the synthesis of ZnSe/ZnS:Mn/ZnS core/shell/shell QDs were determined as follows. (1) First, non-doped ZnSe QDs were synthesised as hosts. (2) The ZnS:Mn shell precursor was prepared at Zn : S : NAC : Mn = 1.0 : 0.2 : 7.2 : 0.15 and adjusted to pH 10.5. (3) Then, the ZnS:Mn precursor was mixed with the previously

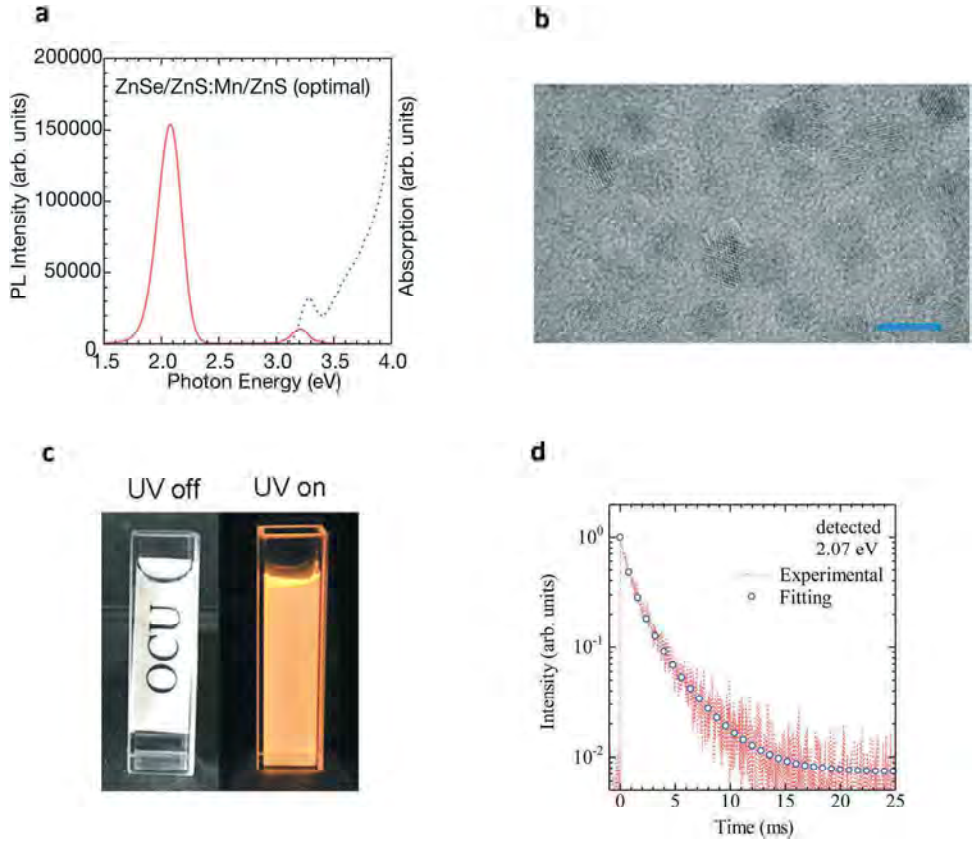

Fig. 4 Properties of the ZnSe/ZnS:Mn/ZnS core/shell/shell QDs. (a) Absorption (blue dashed line) and PL (red solid line) spectra of the ZnSe/ZnS:Mn/ZnS core/shell/shell QDs. (b) TEM image of the ZnSe/ZnS:Mn/ZnS core/shell/shell QDs. The scale bar is 5 nm. (c) ZnSe/ZnS:Mn/ZnS core/shell/shell QD solution under room light and UV irradiation. (d) PL decay profile of the ZnSe/ZnS:Mn/ZnS core/shell/shell QDs.

prepared ZnSe-core QD solution at [ZnS:Mn]/[ZnSe] = 2.0, and ZnSe/ZnS:Mn core/shell QDs were synthesised by microwave irradiation at 120 °C for 2 min. (4) The ZnS precursor was prepared at a Zn : S : NAC molar ratio of 1.0 : 0.2 : 2.4 and adjusted to pH 4.5, then added to the solution from step (3) at [ZnS]/[ZnSe] = 9 and heated at 140 °C for 2 min by microwave irradiation. (5) Finally, to form the ZnS outer shell, the addition of the ZnS precursor and subsequent heating were repeated 5 times. The optimum conditions for the total amount of added [ZnS] were ([ZnS:Mn] + [ZnS])/[ZnSe] = 61.

The absorption and PL spectra of the ZnSe/ZnS:Mn/ZnS core/shell/shell QDs prepared under the optimum conditions are shown in Fig. 4a, illustrating the achieved PLQY of 84%. To the best of our knowledge, this PLQY is the highest reported thus far for water-soluble Mn-doped ZnSe QDs. From the EDX measurements, the Mn concentration in the ZnSe/ZnS:Mn/ZnS QDs, synthesized under optimal conditions, was confirmed to be 1%. A typical transmission electron microscopy (TEM) image is shown in Fig. 4b and c shows photographs of the water-soluble ZnSe/ZnS:Mn/ZnS core/shell/shell QDs under room light and UV excitation. The solution was highly transparent to visible light and showed strong orange emission under UV irradiation. Fig. 4d shows the PL decay profile measured at the PL peak of 2.1 eV for the ZnSe/ZnS:Mn/ZnS QDs. The PL decay profile was fitted using the sum of three single exponential functions $I(t) = \sum A_i \cdot \exp(-t/\tau_i)$, and the average lifetime was calculated using $\langle\tau\rangle = \sum A_i \cdot \tau_i^2 / \sum A_i \cdot \tau_i$.[53] Here, A_i represents the weight of each component. The obtained $\langle\tau\rangle$ was approximately 2.2 ms; this long lifetime of the order of milliseconds was consistent with the intrinsic nature of the intra-3d transition of the Mn dopant.[34,35,53]

By optimising the preparation conditions, we synthesised ZnSe/ZnS:Mn/ZnS core/shell/shell QDs with a wavelength conversion function and maximised PLQY. To apply the water-soluble ZnSe/ZnS:Mn/ZnS QDs to wavelength-conversion materials and improve the conversion efficiency of Si solar cells, the prepared QDs were dispersed in sol–gel glass to fabricate highly luminescent wavelength-conversion glass (Fig. 1b). The higher the QD concentration, the better it would be for the application of the Si solar cells. However, the dispersibility decreased and the QD aggregated when the QD concentration was too high, causing the QD glass to become cloudy, leading to remarkably lowered transmittance. Therefore, the QD concentration was increased within the range wherein white turbidity due to aggregation did not occur. The transmission spectrum of the QD glass is shown in Fig. S4a (ESI†). While the transmittance is close to 90% for visible light (>400 nm), the transmittance decreases sharply for UV light (<400 nm). Additionally, as shown in Fig. S4b (ESI†), the QD glass emits strong orange PL. Thus, we succeeded in fabricating optimal wavelength conversion for Si solar cells.

The QD glass was then applied to a commercially available Si solar cell module. To investigate whether the wavelength-conversion function of the QD glass improves the conversion efficiency, we compared the output characteristics of Si solar cells with and without the QD glass. Fig. S5 (ESI†) shows the surface reflectance of the solar cells before and after applying the QD glass. In the wavelength range from 400 nm to 1200 nm, the reflectance before and after applying the QD glass were the same. In contrast, in the wavelength region below 400 nm, the reflectance increased applying the QD glass. For measuring reflectance, monochromatic light was irradiated onto a sample and the reflected light was detected. Since the reflected light from the sample was directly incident on the photodetector, we considered that PL from the QD glass was detected. Fig. S6 (ESI†) shows the SEM image of the solar cell with the QD glass, which confirms that a flat surface is formed without cracks or visible irregularities. Furthermore, we considered that the flatness of this QD glass ensured its high transmittance.

Fig. 5a shows the *I*–*V* curves of the solar cells. The short-circuit current density (J_{sc}) increased from 42.4 to 43.5 mA cm^{-2} upon adding the QD glass. Furthermore, as shown in the external quantum efficiency (EQE) spectra in Fig. 5b, the solar cell with the QD glass showed a clear increase in EQE in the UV region. Since fluorescent thin films such as the QD glass act as light guide plates, fluorescence is lost from the end face of the glass toward the outside,[54,55] thereby hindering improvements to the solar cell efficiency. Therefore, to further improve the output characteristics of the solar cell by reducing the light loss, Al tape was attached to the side of the solar cell with the QD glass. As shown in Fig. 5a, the J_{SC} increased from 43.5 to 44.4 mA cm^{-2} upon the addition of the Al tape, and as shown in Fig. 5b, the EQE was also increased further. These results demonstrated that the Al tape reduced the loss of light from the end face and improves the power generation efficiency.

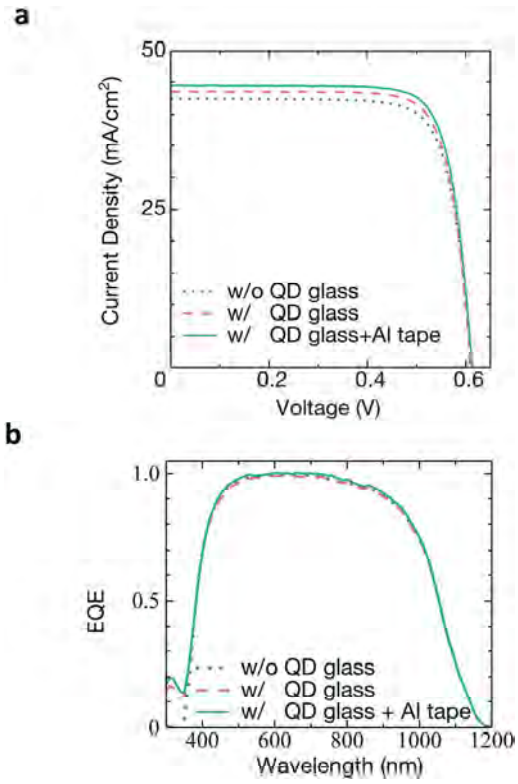

Fig. 5 *I*–*V* characteristics and EQE of Si solar cells with and without the QD glass. (a) *I*–*V* curves under AM1.5G/1 SUN irradiation and (b) EQE spectra of Si solar cells without the QD glass (blue dotted lines), with the QD glass (red dashed lines), and with the QD glass and Al tape (green solid lines). The irradiation light intensity in the *I*–*V* measurement is 100 mW cm^{-2}, and the irradiation light intensity in the EQE measurement is 1.0 mW cm^{-2}.

As a result, the conversion efficiency of the Si solar cell was improved from 20% to 20.7% by adding the QD glass. Furthermore, by suppressing the light loss with the Al tape, the efficiency was improved to 21.5%. Overall, the conversion efficiency of the solar cell with the wavelength-conversion glass and Al tape was improved by 7.4% compared with that of the bare solar cell. The change in EQE was small, relative to the improvement rate of J_{sc} in the *I*–*V* measurements, mainly due to the differences in experimental conditions between the *I*–*V* and EQE measurements. The first reason was the difference in the irradiation light area. The solar cell module used in this study had a Si solar cell area of 10 mm × 10 mm (1.0 cm^2) and a protective glass area of 15 mm × 15 mm (2.25 cm^2). The irradiation area in the EQE measurement was 10 mm × 10 mm, and the Si solar cell was irradiated. During the *I*–*V* measurement, the entire module, including the protective glass, was irradiated. Since the irradiation area was larger in the *I*–*V* measurement, not only the pseudo-sunlight directly incident on the Si solar cell, but also the light emitted from the QD glass outside the solar cell, reaches the Si solar cell. Therefore, the improvement rate of J_{sc} in the *I*–*V* measurements increased. Another difference in the experimental conditions between *I*–*V* and EQE measurements was the difference in irradiation light intensity. The irradiation light intensities during the EQE and *I*–*V* measurements were 1.0 and 100 mW cm^{-2}, respectively. Since the irradiation light intensity in the *I*–*V* measurement was 100 times greater than that in the EQE measurement, the contribution of PL from the aforementioned QD glass in the EQE measurement was increased further, and consequently, the improvement rate of J_{sc} was increased.

The results of the EQE measurements confirm the effect of wavelength conversion by the ZnSe/ZnS:Mn/ZnS QDs. However, it was considered that the improvement in power generation efficiency was due not only to the wavelength conversion function by the QDs, but also to the increase in effective absorption in the Si solar cell coated with the QD glass and with the Al tape. Therefore, it is suggested that the conversion efficiency may be improved further by optimising the device structure, including the wavelength-conversion glass.

Conclusions

In conclusion, water-soluble ZnSe/ZnS:Mn/ZnS QDs with a high PLQY of 84% were synthesised by a hydrothermal method and applied to wavelength-conversion materials to improve the

conversion efficiency of Si solar cells. During the synthesis of the ZnSe/ZnS:Mn/ZnS QDs, non-doped ZnSe QDs were used as hosts, and we focused on Mn^{2+} doping of the shell layer instead of directly doping the core QDs. Additionally, the ZnSe/ZnS:Mn/ZnS QDs were dispersed in sol–gel glass to prepare wavelength-conversion glass. By adding this glass to the top of a solar cell, the power generation efficiency increased by 7.4% (from 20.0% to 21.5%). These results demonstrated that the highly luminescent Mn-doped ZnSe QDs possessed significant potential for application as wavelength-conversion materials.

Conflicts of interest

There are no conflicts to declare.

Acknowledgements

N. S. and D. K. acknowledge a Grant-in-Aid for Scientific Research (B) (No. 17H03538) from the Japan Society for the Promotion of Science (KAKENHI). This work was also supported by the JST OPERA Program (JPMJOP1843).

References

1 E. Placzek-Popko, *Opto-Electron. Rev.*, 2017, **25**, 55–64.
2 M. A. Green, E. D. Dunlop, D. H. Levi, J. Hohl-Ebinger, M. Yoshita and A. W. Y. Ho-Baillie, *Prog. Photovoltaics*, 2019, **27**, 565–575.
3 K. Yoshikawa, H. Kawasaki, W. Yoshida, T. Irie, K. Konishi, K. Nakano, T. Uto, D. Adachi, M. Kanematsu, H. Uzu and K. Yamamoto, *Nat. Energy*, 2017, **2**, 17032.
4 A. Richter, J. Benick, F. Feldmann, A. Fell, M. Hermle and S. W. Glunz, *Sol. Energy Mater. Sol. Cells*, 2017, **173**, 96–105.
5 B. S. Richards, *Sol. Energy Mater. Sol. Cells*, 2006, **90**, 2329–2337.
6 X. Y. Huang, S. Y. Han, W. Huang and X. G. Liu, *Chem. Soc. Rev.*, 2013, **42**, 173–201.
7 B. McKenna and R. C. Evans, *Adv. Mater.*, 2017, **29**, 160649.
8 E. Klampaftis and B. S. Richards, *Prog. Photovoltaics*, 2011, **19**, 345–351.
9 L. Danos, T. Parel, T. Markvart, V. Barrioz, W. S. M. Brooks and S. J. C. Irvine, *Sol. Energy Mater. Sol. Cells*, 2012, **98**, 486–490.
10 A. Solodovnyk, C. Kick, A. Osvet, H. J. Egelhaaf, E. Stern, M. Batentschuk, K. Forberich and C. J. Brabec, *Energy Technol.*, 2016, **4**, 385–392.
11 Y. Iso, S. Takeshita and T. Isobe, *J. Electrochem. Soc.*, 2012, **159**, J72–J76.
12 B. S. Richards, *Sol. Energy Mater. Sol. Cells*, 2006, **90**, 1189–1207.
13 K. Fujita, R. Watanabe, Y. Iso and T. Isobe, *J. Lumin.*, 2018, **198**, 243–250.
14 B. M. van der Ende, L. Aarts and A. Meijerink, *Phys. Chem. Chem. Phys.*, 2009, **11**, 11081–11095.
15 G. Griffini, F. Bella, F. Nisic, C. Dragonetti, D. Roberto, M. Levi, R. Bongiovanni and S. Turri, *Adv. Energy Mater.*, 2015, **5**, 1401312.
16 T. Fukuda, S. Kato, E. Kin, K. Okaniwa, H. Morikawa, Z. Honda and N. Kamata, *Opt. Mater.*, 2009, **32**, 22–25.
17 S. W. Baek, J. H. Shim and J. G. Park, *Phys. Chem. Chem. Phys.*, 2014, **16**, 18205–18210.
18 F. Y. Wang, M. F. Yang, S. H. Ji, L. L. Yang, J. L. Zhao, H. L. Liu, Y. R. Sui, Y. F. Sun, J. H. Yang and X. D. Zhang, *J. Power Sources*, 2018, **395**, 85–91.
19 I. Levchuk, C. Wurth, F. Krause, A. Osvet, M. Batentschuk, U. Resch-Genger, C. Kolbeck, P. Herre, H. P. Steinruck, W. Peukert and C. J. Brabec, *Energy Environ. Sci.*, 2016, **9**, 1083–1094.
20 Q. Wang, X. S. Zhang, Z. W. Jin, J. R. Zhang, Z. F. Gao, Y. F. Li and S. Z. F. Liu, *ACS Energy Lett.*, 2017, **2**, 1479–1486.
21 A. Shalav, B. S. Richards and M. A. Green, *Sol. Energy Mater. Sol. Cells*, 2007, **91**, 829–842.
22 A. Ishii and M. Hasegawa, *Sci. Rep.*, 2017, **7**, 41446.
23 F. Y. Wang, Y. H. Zhang, M. F. Yang, L. L. Yang, Y. R. Sui, J. H. Yang, Y. Zhao and X. D. Zhang, *Adv. Funct. Mater.*, 2018, **28**, 1805001.
24 H. Kataoka, S. Omagari, T. Nakanishi and Y. Hasegawa, *Opt. Mater.*, 2015, **42**, 411–416.
25 U. Resch-Genger, M. Grabolle, S. Cavaliere-Jaricot, R. Nitschke and T. Nann, *Nat. Methods*, 2008, **5**, 763–775.
26 K. D. Wegner and N. Hildebrandt, *Chem. Soc. Rev.*, 2015, **44**, 4792–4834.
27 A. L. Efros, M. Rosen, M. Kuno, M. Nirmal, D. J. Norris and M. Bawendi, *Phys. Rev. B: Condens. Matter Mater. Phys.*, 1996, **54**, 4843–4856.
28 H. B. Bu, H. Yokota, K. Shimura, K. Takahasi, T. Taniguchi and D. Kim, *Chem. Lett.*, 2015, **44**, 200–202.
29 H. Nishimura, Y. X. Lin, M. Hizume, T. Taniguchi, N. Shigekawa, T. Takagi, S. Sobue, S. Kawai, E. Okuno and D. Kim, *AIP Adv.*, 2019, **9**, 025223.
30 H. Nishimura, Y. X. Lin, M. Hizume, T. Taniguchi, N. Shigekawa, T. Takagi, S. Sobue, S. Kawai, E. Okuno and D. Kim, *Chem. Lett.*, 2019, **48**, 1081–1083.
31 D. J. Norris, A. L. Efros and S. C. Erwin, *Science*, 2008, **319**, 1776–1779.
32 S. C. Erwin, L. J. Zu, M. I. Haftel, A. L. Efros, T. A. Kennedy and D. J. Norris, *Nature*, 2005, **436**, 91–94.
33 L. R. Bradshaw, K. E. Knowles, S. McDowall and D. R. Gamelin, *Nano Lett.*, 2015, **15**, 1315–1323.
34 C. L. Gan, Y. P. Zhang, D. Battaglia, X. G. Peng and M. Xiao, *Appl. Phys. Lett.*, 2008, **92**, 241111.
35 X. L. Yang, C. D. Pu, H. Y. Qin, S. J. Liu, Z. A. Xu and X. G. Peng, *J. Am. Chem. Soc.*, 2019, **141**, 2288–2298.
36 C. L. Li and N. Murase, *Langmuir*, 2004, **20**, 1–4.
37 H. B. Bu, T. Watanabe, M. Hizume, T. Takagi, S. Sobue, S. Kawai, E. Okuno and D. Kim, *Mater. Res. Express*, 2015, **2**, 036202.
38 S. Jun, J. Lee and E. Jang, *ACS Nano*, 2013, **7**, 1472–1477.
39 Y. Liu, D. D. Yu, W. Zhu, X. Bai, Q. H. Shen, X. Y. Liu and J. G. Zhou, *Chem. Res. Chin. Univ.*, 2017, **33**, 327–332.

40 X. Michalet, F. F. Pinaud, L. A. Bentolila, J. M. Tsay, S. Doose, J. J. Li, G. Sundaresan, A. M. Wu, S. S. Gambhir and S. Weiss, *Science*, 2005, **307**, 538–544.

41 P. Reiss, J. Bleuse and A. Pron, *Nano Lett.*, 2002, **2**, 781–784.

42 J. Selyaraj, A. Mahesh, V. Asokan, V. Baskaralingam, A. Dhayalan and T. Paramasivam, *ACS Appl. Nano Mater.*, 2018, **1**, 371–383.

43 A. Aboulaich, M. Geszke, L. Balan, J. Ghanbaja, G. Medjahdi and R. Schneider, *Inorg. Chem.*, 2010, **49**, 10940–10948.

44 M. Hardzei and M. Artemyev, *J. Lumin.*, 2012, **132**, 425–428.

45 Y. S. Lee, K. Nakano, H. B. Bu and D. G. Kim, *Appl. Phys. Express*, 2017, **10**, 065001.

46 Y. S. Lee, H. B. Bu, T. Taniguchi, T. Takagi, S. Sobue, H. Yamada, T. Iwaki and D. Kim, *Chem. Lett.*, 2016, **45**, 878–880.

47 L. H. Jing, S. V. Kershaw, Y. L. Li, X. Huang, Y. Y. Li, A. L. Rogach and M. Y. Gao, *Chem. Rev.*, 2016, **116**, 10623–10730.

48 G. M. Dalpian and J. R. Chelikowsky, *Phys. Rev. Lett.*, 2006, **96**, 226802.

49 P. Wu and X. P. Yan, *Chem. Soc. Rev.*, 2013, **42**, 5489–5521.

50 V. Wood, J. E. Halpert, M. J. Panzer, M. G. Bawendi and V. Bulovic, *Nano Lett.*, 2009, **9**, 2367–2371.

51 R. Thakar, Y. C. Chen and P. T. Snee, *Nano Lett.*, 2007, **7**, 3429–3432.

52 B. T. Luong, E. Hyeong, S. Ji and N. Kim, *RSC Adv.*, 2012, **2**, 12132–12135.

53 C. D. Pu, J. L. Ma, H. Y. Qin, M. Yan, T. Fu, Y. Niu, X. L. Yang, Y. F. Huang, F. Zhao and X. G. Peng, *ACS Cent. Sci.*, 2016, **2**, 32–39.

54 G. C. Glaeser and U. Rau, *Thin Solid Films*, 2007, **515**, 5964–5967.

55 E. Klampaftis, D. Ross, K. R. McIntosh and B. S. Richards, *Sol. Energy Mater. Sol. Cells*, 2009, **93**, 1182–1194.